Available online at www.sciencedirect.com
SCIENCE DIRECT®
International Journal of Heat and Mass Transfer 49 (2006) 1462–1471
International Journal of HEAT and MASS TRANSFER
www.elsevier.com/locate/ijhmt

Experimental study of heat transfer enhancement in a drag-reducing two-dimensional channel flow

T. Zhou *, K.C. Leong, K.H. Yeo

School of Mechanical and Aerospace Engineering, Nanyang Technological University, 50 Nanyang Avenue, Singapore 639798, Republic of Singapore

Received 2 March 2005; received in revised form 10 September 2005
Available online 23 November 2005

Abstract

In this paper, drag reduction and heat transfer enhancement were studied in a fully developed two-dimensional water channel flow. Surfactant solutions at different concentrations, namely 30, 70, 80 and 90 ppm, were used to examine the influence of surfactant additives on the skin friction drag and heat transfer coefficient. The magnitudes of the maximum achievable drag reduction at the above four different surfactant concentrations are about 7%, 30%, 50% and 55%, respectively. The present results show that there is no heat transfer reduction when 30 ppm of surfactant is added to the flow. With the increase of surfactant concentration to 90 ppm, heat transfer rate was reduced by about 55%. The critical Reynolds number for loss of heat transfer reduction increases with the increase of surfactant concentration. The effect of the low-profile vortex generators on heat transfer rate was examined for the surfactant concentration of 90 ppm. The results show that the averaged Nusselt number is enhanced by 180%, 160% and 150% for the Reynolds numbers of 7000, 12,000 and 16,200, respectively, as compared with that obtained in the surfactant solution without the use of vortex generators and yet the pressure drop penalty for heat transfer enhancement is rather small.

Keywords: Heat transfer enhancement; Drag reduction; Vortex generator

1. Introduction

Since the discovery of the Toms effect [1], polymers as drag-reducing additives are well recognized. They have been used widely to reduce the undesired drag that occurs in long-distance transportation of liquids. However, less attention has been focused recently on the use of polymers as drag-reducing additives, especially for re-circulating flow systems. This is because the polymer's capability as a drag reducer can be permanently crippled when it is subjected to high shear stress or when exposed to prolonged periods of turbulent flow and repeated heating and cooling regions. In contrast to polymers, the mechanical degradation of surfactants is only temporary [2]. Surfactants have the ability to restructure its rod-like microstructures and re-assume its own drag-reducing capability when the shear stress in the flow decreases to a certain level. The orientation of the large-scale orderly rod-like micelle structures, which promote the drag reduction phenomenon, is recoverable on the order of seconds even after being disrupted [3].

In addition to the drag-reducing effect, another noticeable effect of drag-reducing additives is the heat transfer reduction that occurs between a solid boundary and the flowing fluid [3–9]. According to Cho and Hartnett [5] and Gasljevic and Matthys [6], some drag-reducing additives can result in a heat transfer reduction which is much larger than the drag reduction. Heat transfer reduction is desired in the distribution pipelines of a district heating/cooling system because it lowers the requirement on insulation along the pipelines. However, this phenomenon is undesired in some cases, such as in the heat exchanger and the chiller because it will deteriorate their heat transfer

* Corresponding author. Tel.: +65 6790 4331; fax: +65 6792 4612.
E-mail address: mtmzhou@ntu.edu.sg (T. Zhou).

0017-9310/$ - see front matter © 2005 Elsevier Ltd. All rights reserved.
doi:10.1016/j.ijheatmasstransfer.2005.09.023

Nomenclature

c	concentration of surfactant solution (ppm)
C_f	Fanning friction factor
D	hydraulic diameter (m)
DR	drag reduction (%)
H	height of the water channel (m)
h_x	local heat transfer coefficient (W m^{-2} K^{-1})
HTR	heat transfer reduction (%)
k	thermal conductivity of water (W m^{-1} K^{-1})
L	length of the heating surface (m)
Nu_x	local Nusselt number
ppm	parts per million mass
Pr	Prandtl number of water
q''_s	local heat flux (W m^{-2})
Re	Reynolds number based on the height of the channel, $\equiv U_b H/v$
Re_{cri}	critical Reynolds number for drag and heat transfer reduction
T_b	local bulk temperature of the flow above the heating surface (K)
U_b	bulk velocity (m/s)
u_*	friction velocity (m/s)
x	distance measured from the leading edge of the heating surface (m)

Greek symbols

v	kinematic viscosity of water (m^2 s^{-1})
ρ	density of water (kg m^{-3})
τ_w	shear stress on the wall surface of the rectangular duct (N m^{-2})

Subscripts

w	quantities obtained in water
s	quantities obtained in surfactant solution

capability. The latter effect will reduce the overall performance of the system [7]. In recent years, many researchers [10–15] have begun to realize this issue and paid much attention to the investigation of enhancement techniques for heat transfer in drag-reducing flows. Typically, there are two different approaches to enhance the heat transfer rate between a solid boundary and the fluid, namely the passive and the active methods. Fossa and Tagliafico [10] carried out an experimental study in a single-pipe type counter-current heat exchanger of 0.6 m in length, in which chilled dilute polymer solution flows in the external annular duct. The annular passage for the chilled drag-reducing solution consists of an outer pipe that has an internal smooth surface and an inner pipe that can have either a smooth, finned or grooved outer surface. With this set up, they found that the heat transfer rate was not recovered to the magnitude obtained in pure water flow. Thus, it is not a good enhancement method in the drag-reducing flow. Another work for heat transfer enhancement in a drag-reducing flow was carried out by Qi et al. [11]. In their study, drag reduction and heat transfer reduction and enhancement tests in a fluted tube-in-tube heat exchanger with four starts were conducted for cationic surfactant solution Ethoquad T13-50/NaSal (5 mM/8.75 mM) and zwitterionic/anionic surfactant solution SPE98330 (1500 ppm). The outer surface of the heat exchanger was well insulated to prevent heat loss. While chilled water or drag-reducing fluid flows through the annulus of the heat exchanger, shear stress is enhanced with the aid of the embedded spiral starts. As a result, the super-ordered micelle structures in the surfactant solution are broken down. They found that for Re in the range of 10,000–50,000 and the test fluid inlet temperature in the range of 50–70 °C, the fluted inner tube heat exchanger can increase the heat transfer coefficients for both cationic and zwitterionic/anionic drag-reducing fluids. While the pressure drop penalty for the cationic surfactant solution is high, it is only modest for the zwitterionic/anionic solution. A passive heat transfer enhancement technique was also investigated by Li et al. [12]. Their investigation, which involved the use of three types of wire meshes, was conducted in a 6-m-long water tunnel with cross-section of 500 mm (width) × 40 mm (height). The wire-mesh was installed upstream of the heating section. It served as a high shear stress inducer to destroy the rod-like micelle structures in the surfactant solution. Eschenbacher et al. [13] used a single wing-type vortex generator to generate a longitudinal vortex in the drag-reducing flow. The vortex generator with a delta-shaped winglet was made of brass and was attached to the bottom wall of the test section of a rectangular duct. It had an angle of attack against the main flow of 30°. The height of the trailing edge was $0.5H$ and the base length was set equal to $2H$, where H is the height of the tunnel. It was found that the heat transfer coefficient of the surfactant solution was enhanced to the same value as that for water. Qi et al. [15] used static mixers and honeycombs to enhance heat transfer rate of drag-reducing fluid in a heat exchanger. They found that the 15 elements of mixers is the best device to enhance the heat transfer rate with a modest pressure drop. However, the practical application of the honeycombs is restricted due to its small effect on heat transfer enhancement even though the pressure drop penalty caused by the honeycombs is low.

Numerous experimental studies have been carried out to actively control turbulent flow and its concomitant transport phenomena such as friction drag and heat transfer [16–18]. The most successful method to date is the so-called "synthetic jet" [18]. By using the synthetic jet technique, Glezer [19] carried out boundary layer separation control and virtual-shaping of airfoils. Flow control investigations

were also performed numerically by many investigators [20–22]. Robinson [23] observed that the streamwise vortices in the boundary layer are responsible for the "ejection" and "sweep" events of the bursting process. Recent studies have also shown that the high skin-friction regions are closely related to the streamwise vortices in the boundary layer. These near-wall streamwise vortices are the most relevant structures for drag reduction in turbulent boundary layers [20–22]. Therefore, significant drag reduction is possible if the near-wall streamwise vortices can be suppressed [20,21].

The present study aims to enhance the heat transfer rate over a heating surface in a drag-reducing flow by using a row of low-profile vortex generators at different Reynolds numbers. The Nusselt numbers measured downstream of the vortex generators will be compared with those obtained before the use of the vortex generators. Dependences of drag reduction on Reynolds numbers and surfactant concentrations will also be examined.

2. Experimental setup

The present experiments were conducted in a closed-loop two-dimensional water channel flow (Fig. 1). The dimensions of the channel are 0.5 m (width) × 0.05 m (height) and 6 m (length). Honeycomb rectifiers were used both in the upstream water tank and at the entrance of the channel to remove the large eddies in the flow. A heating plate with a surface area of 0.4 m (width) × 0.6 m (length) was installed flush with the bottom wall of the test section. Beneath the heating plate, 12 K-type thermocouples were installed in a straight-line along the streamwise direction. All these thermocouples were connected to a PC-based data acquisition system. During the experiments, a direct-current electrical power supply was employed to deliver a constant power of 315 W to the heater. A voltmeter and an ammeter were used to measure the input voltage and current, respectively. The heat transfer coefficients were determined through the measurements of the power input to the heater and the temperature distribution on the heating surface. These measured parameters were converted to local Nusselt numbers to quantify the heat transfer rate. Untreated tap water was used as the working fluid. The temperature of the tap water was maintained at about 29 °C (±1 °C) by a chiller. Cetyltrimethyl ammonium chloride (CTAC) and NaSal were pre-mixed (the proportion for CTAC/NaSal mixture is 0.5 in terms of molar ratios) with de-ionized water and stirred in a container with a magnetic stirrer for 2 h before it was charged into the re-circulating system. It was also found that the drag reduction effect of the fresh solution decayed with time until the fourth day after the preparation. Therefore, the fresh surfactant solution was allowed to rest for 4 days before measurements were conducted.

An electromagnetic flow meter was used to measure the volume flow rate in the water channel. The wall shear stress was calculated from the static pressure gradient measured along the channel. To reduce the uncertainty in measuring the pressure gradient, pressure differences between a series of static pressure tapping points located at an interval of 0.3 m on the top wall of the water channel and the reference pressure (located at the exit section of the channel, as shown in Fig. 1) were measured using a pressure transducer (Druck LPM 5000 Series). The first pressure-tap-point is located at 60 mm away from the entrance. The pressure transducer has a pair of pressure-signal ports. One of the ports (low-pressure port) was connected permanently to a reference pressure tapping point located at 5.46 m downstream from the channel entrance while the other port (high-pressure port) was connected individually to the pressure-line-selecting switch. This switch was installed between the pressure transducer and the water

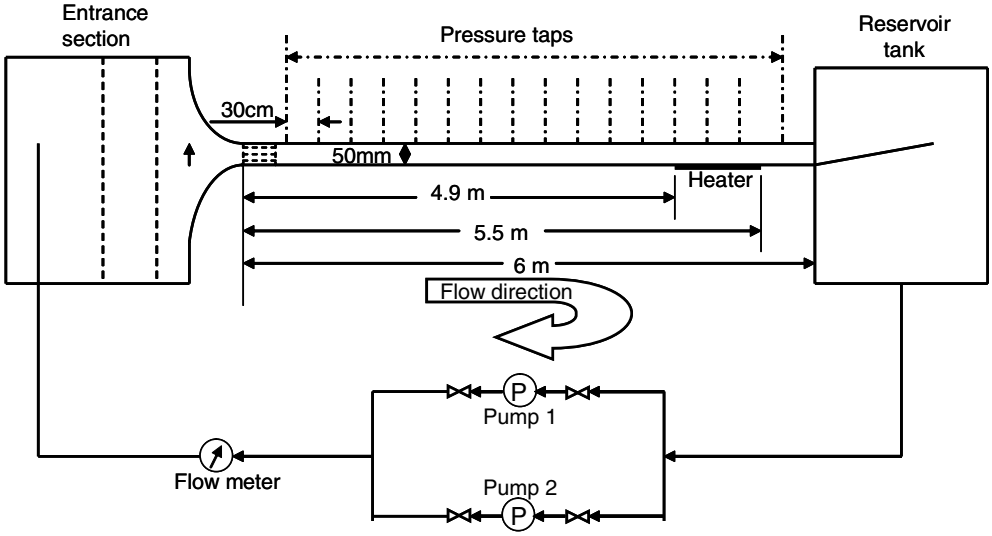

Fig. 1. Schematic diagram of the two-dimensional water channel flow. The dashed lines represent honeycomb. The dash-dotted lines are for pressure difference measurements between two tapping points along the channel.

tunnel to enable selection of signal-line from the multiple pressure-tap points on the tunnel. The pressure-line-selecting switch is basically an enclosed cylindrical vessel with an outlet, a row of inlet ports for pressure signals and a purging port. The function of the outlet port is to transmit selected the pressure signals to the pressure transducer. The row of inlet ports was used to tap pressure signals from various pressure-tapping points along the duct. Air bubbles in the pressure-signal transmitting lines were removed through the purging port. Pressure drop over the heating surface due to the use of the vortex generators was also measured to assess the pressure drop penalty. One of the two tapping points is located 0.2 m upstream while the other is located 0.2 m downstream of the vortex generators.

A row of low-profile vortex generators (Fig. 2) with height of 6 mm installed at $x/H = 5$ mm from the leading edge of the heating surface and aligned in the spanwise direction were used to enhance heat transfer in the drag-reducing flow. The practical advantages of these vortex generators are their inherent simplicity and low device drag [24–26]. According to previous studies [25,26], the most effective vortex generators that are able to produce longitudinal vortices with low pressure loss would have a height between 10% and 35% of the boundary-layer thickness at the device installation location.

The experimental uncertainty for the Fanning friction factor C_f was estimated using the propagation of random uncertainty technique proposed by Kline and McClintock [27]. The results show that the relative uncertainty of C_f decreases with Reynolds number, changing from 14.9% at $Re = 7000$ to 4.1% at $Re = 18{,}500$, while the uncertainty for Nu increases with Reynolds number, changing from 8% at $Re = 7000$ to 15.5% at $Re = 18{,}500$.

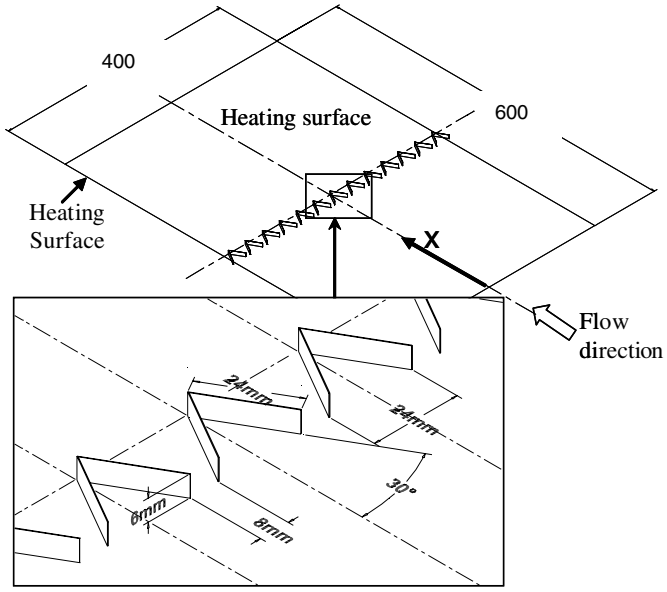

Fig. 2. Co-ordinate system and schematic diagram of the low-profile vortex generators on the heating surface.

3. Results and discussion

3.1. Drag reduction

For a fully developed turbulent channel flow, Tennekes and Lumlay [28] have shown that

$$u_*^2 = -\frac{H}{2\rho} \times \frac{\mathrm{d}p}{\mathrm{d}x}, \tag{1}$$

where $u_* \equiv \sqrt{\tau_w/\rho}$ is the friction velocity. Since u_* does not change in the streamwise direction in a fully developed turbulent channel flow, $\mathrm{d}p/\mathrm{d}x$ should be a constant. The Fanning friction factor, C_f, is related with the wall shear stress τ_w via.

$$C_f = \frac{\tau_w}{\rho \times U_b^2/2}. \tag{2}$$

Therefore, by measuring the flow rate and the pressure gradient $\mathrm{d}p/\mathrm{d}x$ in the channel, C_f can be calculated. The drag reduction, DR, is defined as the difference between the values of the Fanning friction factor for water and for the surfactant solution at the same Reynolds number, divided by the value for water. This is normally expressed in terms of a percentage:

$$\mathrm{DR} = \frac{C_{fw} - C_{fs}}{C_{fw}} \times 100\%, \tag{3}$$

where C_{fw} and C_{fs} are the Fanning friction factors for water and surfactant solution, respectively. Unlike in a Newtonian fluid flow where the friction coefficient depends only on Reynolds number, the friction coefficient in a drag-reducing fluid depends also on the dimension of the carriers of the flow [29,30].

The Fanning friction factors for four different surfactant concentrations, namely 30, 70, 80 and 90 ppm were measured over the Reynolds number range of 7000–18,500. The values of drag reduction for different surfactant concentrations and at different Reynolds numbers are shown in Fig. 3. The peak values at various concentrations represent the maximum drag reduction. The drag reduction for surfactant concentration of 30 ppm is about 7% at $Re = 7500$. It disappears completely when Re is increased to around 17,000. With 70 ppm of surfactant in the flow, the maximum drag reduction is about 30%. The critical Reynolds number, Re_{cri}, at which the drag starts to recover, increases to approximately 12,000. From the trend for 70 ppm, drag reduction is not expected for $Re > 19{,}000$. With further increase in the surfactant concentration to 80 ppm, significant drag reduction occurs. The maximum achievable drag reduction increases to about 50% at $Re = 15{,}000$. However, with further increase in the surfactant concentration to 90 ppm, the drag reduction does not change appreciably. The maximum achievable drag reduction increases to only about 55% at $Re = 17{,}000$. The critical Reynolds number, Re_{cri}, increases with the increase of surfactant concentration. For example, $Re_{cri} \approx 12{,}000$ at 70 ppm. The magnitude of Re_{cri} increases to 15,000 and

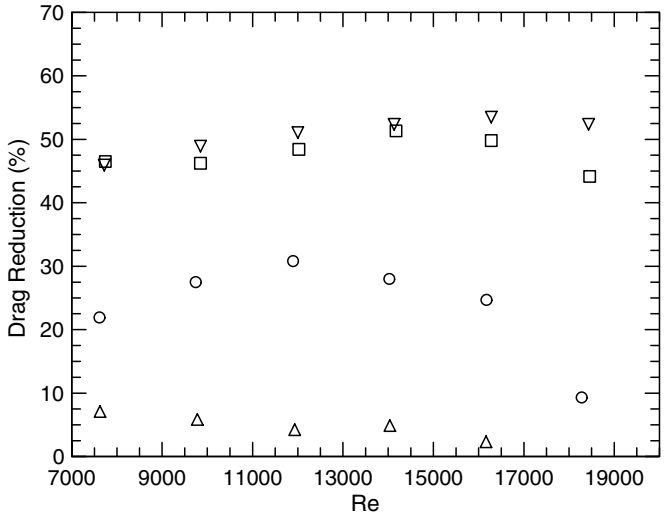

Fig. 3. Dependence of drag reduction on Reynolds numbers. △, 30 ppm; ○, 70 ppm; □, 80 ppm; ▽, 90 ppm.

17,000 for surfactant concentrations of 80 and 90 ppm, respectively. This is consistent with the results obtained by Li et al. [31]. As explained by Ohlendorf et al. [32], an increase in surfactant concentration will lead to an increase in the length of the rod-like micelles that will align themselves along the flow direction to suppress turbulent flow near the wall. As a result, the skin friction between the flowing fluid and the solid boundary is reduced. Thus, when the surfactant concentration in the fluid is higher, the rod-like micelle structures will become longer, resulting in a larger drag reduction and a higher critical Reynolds number. Therefore, a larger amount of energy from the flow is required to disrupt the super-order rod-like micelle structures.

3.2. Heat transfer reduction

The heat transfer over the heating surface is quantified by the local Nusselt number,

$$Nu_x = \frac{h_x \times H}{k}, \tag{4}$$

where k is the thermal conductivity of water and h_x is the local heat transfer coefficient, which can be obtained via.

$$h_x = \frac{q''_s}{T_s - T_b}, \tag{5}$$

where q''_s is the local heat flux, and T_s and T_b are the local temperature of the heating surface and the bulk fluid, respectively. The averaged Nusselt number is calculated based on the averaged heat transfer coefficient which is obtained by integrating the local heat transfer coefficient over a distance x measured from the leading edge of the heating surface.

The heat transfer reduction (HTR) is commonly defined as the difference between the values of the Nusselt numbers for water and for surfactant solution at the same Reynolds number divided by the value for water [6,11,31]. It is expressed in terms of a percentage:

$$\mathrm{HTR} = \frac{Nu_w - Nu_s}{Nu_w} \times 100\%, \tag{6}$$

where Nu_w is the Nusselt number for water and Nu_s is the Nusselt number for surfactant solution. Prior to the study of the heat transfer reduction and enhancement in drag-reducing flow, heat transfer coefficients in the channel flow with tap water at temperature of 29 °C were obtained to establish a benchmark for comparison. The average Nusselt numbers at different Reynolds numbers are shown in Fig. 4. In addition, Gnielinski's [33] result given by Eq. (7) is also included for comparison.

$$Nu_m = 0.012 \times (Re^{0.87} - 280) \times Pr^{0.4} \times \left(1 + \left[\frac{D}{L}\right]^{0.667}\right), \tag{7}$$

where D is the hydraulic diameter and L is the length of the heating surface. Eq. (7) is commonly used to predict the average heat transfer coefficients for turbulent flows of high Prandtl number Pr in smooth channels when the flow condition is thermally and hydrodynamically developed.

In the present experiments, the average Nusselt numbers obtained without surfactant additives agree reasonably well with Gnielinski's [33] equation for Reynolds numbers in the range of 7000–14,000. As the Reynolds number increases, which corresponds to an increase in fluid bulk velocity and hence an increase in velocity fluctuation, heat transfer also increases. The presence of turbulent flow in the wall region would induce better mixing between low-speed region close to the wall and the high-speed region of the main stream. The increase in the mixing of fluid encourages the transfer of heat energy from the wall surface to the main stream. As the Reynolds number is further

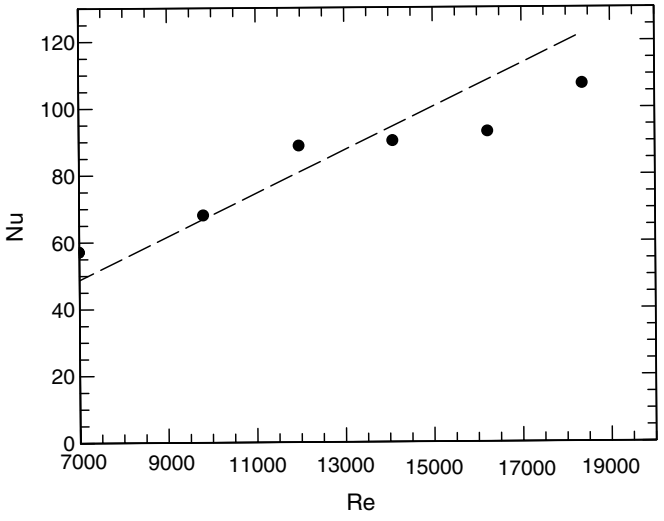

Fig. 4. Averaged Nusselt number at various Reynolds numbers in tap water. ●, Present results; — —, Gnielinski [33] (Eq. (7)).

increased to above 14,000, the average Nusselt numbers deviate slightly from Gnielinski's results.

The heat transfer reduction experiments were performed with surfactant concentrations of 30, 70, 80 and 90 ppm. For each concentration, the experiments were conducted at Reynolds numbers of 7000, 12,000, 16,200 and 18,500, respectively. At $Re = 7000$ (Fig. 5), there is no apparent (within 6%) reduction of heat transfer for 30 ppm of surfactant concentration over the region of $x/H > 3$. This may be due to an earlier occurrence of the critical Reynolds number for the present heat transfer reduction at this concentration. The dramatic heat transfer reduction may have occurred at a Re lower than 7000. It may also be due to the degradation of surfactant aggregation near the wall, which helps to reduce mass exchange in the vertical direction, although experimental system errors may not be completely ruled out. The microstructures of the micelles may be destroyed by the heating effect in the test section as the aggregation of the surfactant micelles depends strongly on the fluid temperature [31]. At the surfactant concentration of 70 ppm, there is a slight (18%) heat transfer reduction over the region of $x/H > 3$. The thermal developing region ends at around $x/H = 3$. Beyond this location, the local Nusselt number remains constant. By increasing the surfactant concentration in the flow to 80 ppm, significant heat transfer reduction is noted. The heat transfer reduction increases to about 45% for $x/H \geqslant 6$. When the surfactant concentration is further increased to 90 ppm, the magnitude of Nu decreases slightly. The small difference between the local Nu at 90 ppm and that at 80 ppm may be within the experimental uncertainty. This result indicates that the heat transfer reduction at $Re = 7000$ may have reached its maximum attainable value. Thus, further heat transfer reduction is not observed even with higher concentrations of surfactant additives in the fluid.

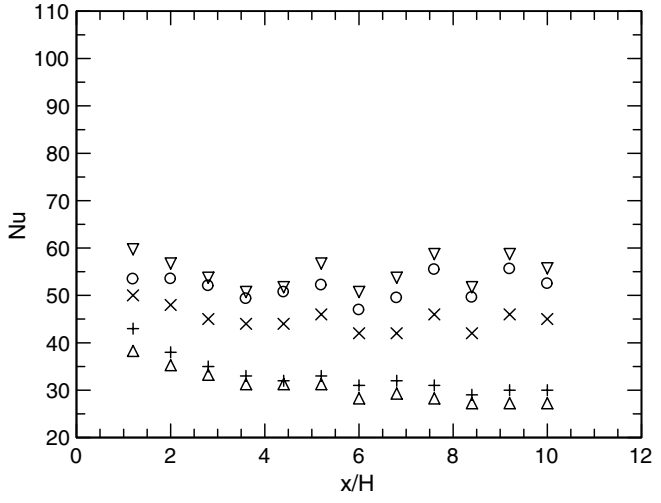

Fig. 5. Comparison of local Nusselt number of water and surfactant solutions at $Re = 7000$. ▽, 0 ppm; ○, 30 ppm; ×, 70 ppm; +, 80 ppm; △, 90 ppm.

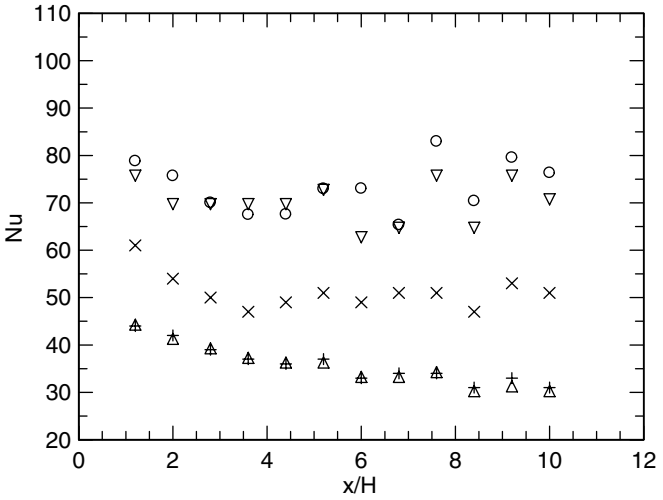

Fig. 6. Comparison of local Nusselt number of water and surfactant solutions at $Re = 12{,}000$. ▽, 0 ppm; ○, 30 ppm; ×, 70 ppm; +, 80 ppm; △, 90 ppm.

When $Re = 12{,}000$ (Fig. 6), there is no apparent heat transfer reduction with surfactant concentration of 30 ppm. The result at this concentration agrees well with that at 0 ppm. This may be because the orderly rod-like microstructures are broken into sphere-like structures at this Reynolds number, which do not have the ability to suppress turbulence on the heating surface. However, when 70 ppm of surfactant concentration is used, the magnitude of the local Nu dropped significantly (by about 32%). With higher concentration of surfactant in the flow, the aggregation forces between the surfactant molecules become stronger. Hence, the rod-like microstructures are able to sustain themselves in the flow and to suppress the mixing effect near the heating surface. By increasing the surfactant concentration in the flow to 80 ppm, a reduction of heat transfer rate of 55% is noted. However, when the surfactant concentration is increased to 90 ppm, no further reduction of heat transfer is observed. The magnitude of the local Nusselt number at 90 ppm agrees well with that at 80 ppm. This may be due to the reason that the flow has reached its maximum attainable heat transfer reduction at $Re = 12{,}000$. Thus, further reduction of heat transfer is not possible even with higher concentration of the surfactant additives. The results in Fig. 6 also indicate that with the increase in surfactant concentration, there is a delay in the establishment of fully developed thermal boundary condition. For example, the thermal boundary layer only becomes fully developed after $x/H = 3$ at 70 ppm. When the surfactant concentration is increased to 80 or 90 ppm, the thermal developing region extends to about $x/H = 8$. This phenomenon is expected, as Gasljevic and Matthys [34] previously highlighted that the thermal developing region in drag-reducing flows is usually significantly longer than those for Newtonian fluids. They claimed that the developing region in a pipe flow with surfactants can go up to $L/D = 1000$, where L is the length of the thermal developing regions and D is the diameter of the pipe.

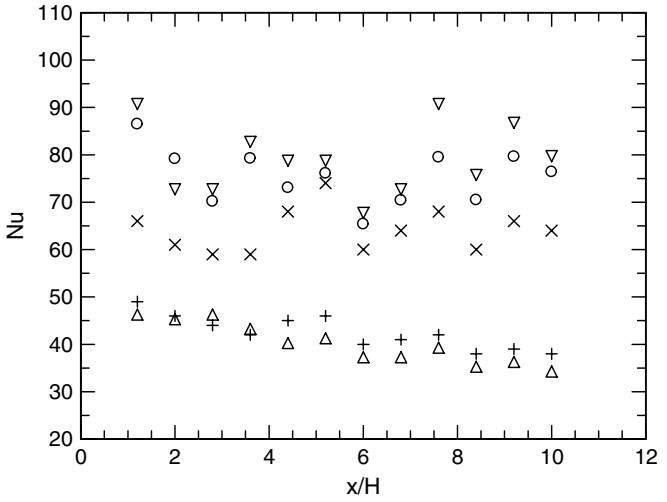

Fig. 7. Comparison of local Nusselt number of water and surfactant solutions at $Re = 16{,}200$. ▽, 0 ppm; ○, 30 ppm; ×, 70 ppm; +, 80 ppm; △, 90 ppm.

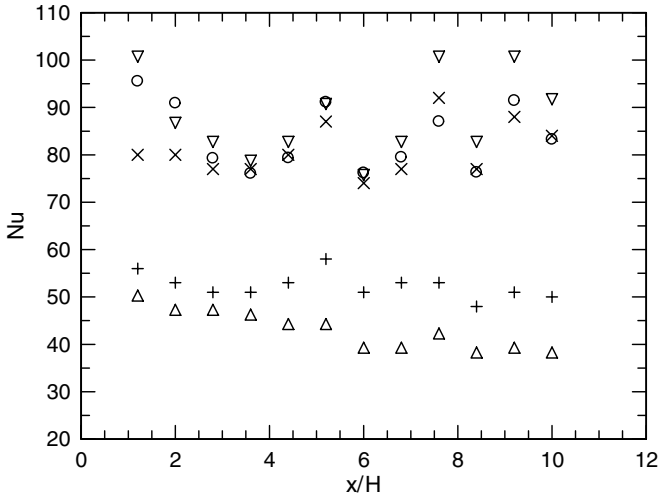

Fig. 8. Comparison of local Nusselt number of water and surfactant solutions at $Re = 18{,}500$. ▽, 0 ppm; ○, 30 ppm; ×, 70 ppm; +, 80 ppm; △, 90 ppm.

When Re is increased to 16,200 (Fig. 7), the distributions of the local Nu for the cases of 0 and 30 ppm scatter significantly. Similar to the previous two Reynolds number cases ($Re = 7000$ and 12,000), the magnitudes of the Nu averaged over $x/H \geqslant 3$ for both 0 and 30 ppm are comparable. For the case of 70 ppm surfactant concentration, there is a reduction of 25% for heat transfer rate over the region of $x/H \leqslant 2$–6. For $x/H > 6$, the heat transfer coefficient starts to increase. This may be due to the breakdown of the rod-like microstructures which are unable to withstand the shear stress from the higher flowrate and the heating effect near the wall. However, when 80 ppm of surfactant is present in the flow, the local Nu decreases significantly by about 45%. With higher concentration of surfactant in the flow, the aggregation forces between the surfactant molecules become larger. As a result, the rod-like microstructures are able to sustain themselves in the flow. When the surfactant concentration is increased to 90 ppm, no further increase in heat transfer reduction was observed. The heat transfer reduction remains at about 45%.

When Re is increased to 18,500 (Fig. 8), the reduction of the local Nu with surfactant concentration of 70 ppm is only seen for $x/H \leqslant 3$. For $x/H > 3$, the differences between Nu obtained at surfactant concentrations of 0 ppm, 30 ppm and 70 ppm are within experimental uncertainty. For the case of 80 ppm surfactant concentration, a heat transfer reduction of about 40% is observed for $x/H > 4$, where the thermal boundary layer is fully developed. At 90 ppm surfactant concentration, the thermal developing region is extended to $x/H = 6$. A reduction of heat transfer rate of about 55% is obtained. Based on the results at surfactant concentration of 80 ppm and 90 ppm for $Re = 18{,}500$, it is difficult to conclude that the maximum attainable heat transfer reduction is achieved as there is a possibility for further heat transfer reduction if the surfactant concentration is increased beyond 90 ppm.

3.3. Heat transfer enhancement

Heat transfer in the drag-reducing flow is enhanced by a row of low-profile vertex generators installed at $x/H = 5$ from the leading edge of the heating surface and aligned in the spanwise direction. Flow visualization (results are not given here) shows that the vortex generators can create an array of longitudinal spiraling vortices. A sketch of the longitudinal vortices downstream of the vortex generators is given in Fig. 9. These vortices help to disrupt the orientation of the orderly aligned micelle structures. Since the longitudinal vortices, which rotate counter-clockwise to their neighboring vortices, promote large-scale motion of fluid between the main stream and the near-wall region, a series of suction fields that draw in cold fluid from the main stream into the near wall region to absorb heating energy are created. The cold fluid will not remain in the near-wall region for long. Immediately after it comes into contact with the hot surface, it will be carried away by the spiraling longitudinal vortices and ejected into the main stream

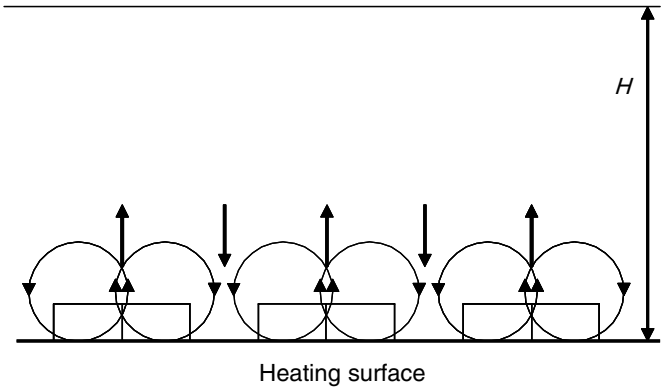

Fig. 9. Sketch of the longitudinal vortices viewed from the end of the test section.

again. This bulk exchange activity helps to transfer heat energy away from the heating surface at a higher rate, resulting in local heat transfer enhancement. The local heat transfer coefficients were determined for $x/H \geqslant 5$ in the streamwise direction. The results obtained at 90 ppm surfactant concentration with Reynolds numbers of 7000, 12,000 and 16,200, respectively, are shown in Fig. 10. Results obtained at 0 and 90 ppm surfactant concentrations without the vortex generators are also shown in Fig. 10 for comparison.

At $Re = 7000$ (Fig. 10a), the Nu averaged over $x/H =$ 5–10 at 90 ppm surfactant concentration with vortex generators is about 180% higher than that obtained without vortex generators. It is also 52% higher than that for tap water without the use of the vortex generators. The maximum attainable Nusselt number changes from 30 to about 87, with the latter value being much higher than the value obtained by Gnielinski [33] in a fully developed channel flow, where a value of 55 was reported. The significant increase in heat transfer rate is related to the streamwise vortices generated by the vortex generators, resulting in the enhanced bulk exchange of fluid between the main flow and the near-wall region. It may also be related to the increased shear stress near the wall due to the constricted passages, which destroys the alignments of the micelle structures.

When Re is increased to 12,000 (Fig. 10b), the maximum local Nu for 90 ppm with vortex generators increases to about 95. The values of Nu averaged over the region of $x/H = 5$–10 is about 160% higher than that obtained without the use of the vortex generators. This result indicates that the heat transfer rate downstream of the vortex generators increases with the increase of Reynolds number. The heat transfer coefficient with the vortex generators is about 22% higher than that in tap water, which is much lower than for the case at $Re = 7000$.

For $Re = 16{,}200$ (Fig. 10c), the values of Nu averaged over $x/H = 5$–10 with vortex generators in 90 ppm increases further to about 98, which is about 150% higher than that obtained without the vortex generators. This value is about 25% higher than that in tap water. This result seems to suggest that the performance of the vortex generators in 90 ppm surfactant solution relative to tap water flow decreases slightly with the increase of Reynolds number.

The results presented in the form of local Nu in Fig. 10 show the deterioration of heat transfer enhancement in the streamwise direction. It is noted that the enhancement to the heat transfer rate of the low-profile vortex generators is not applicable for all downstream locations. For instance at $x/H = 7$ in Fig. 10a, the heat transfer enhancement starts to decline. The location of the onset of this decline shifts further downstream with an increase in Reynolds number. For example, at $Re = 16{,}200$ (Fig. 10c), the onset of decline in heat transfer enhancement starts only at $x/H = 8.4$. The decline of heat transfer enhancement may be related to the loss of the spiraling momentum that sustains the longitudinal vortices in the channel downstream of the vortex generators. It may also be due to the relief of the increased shear

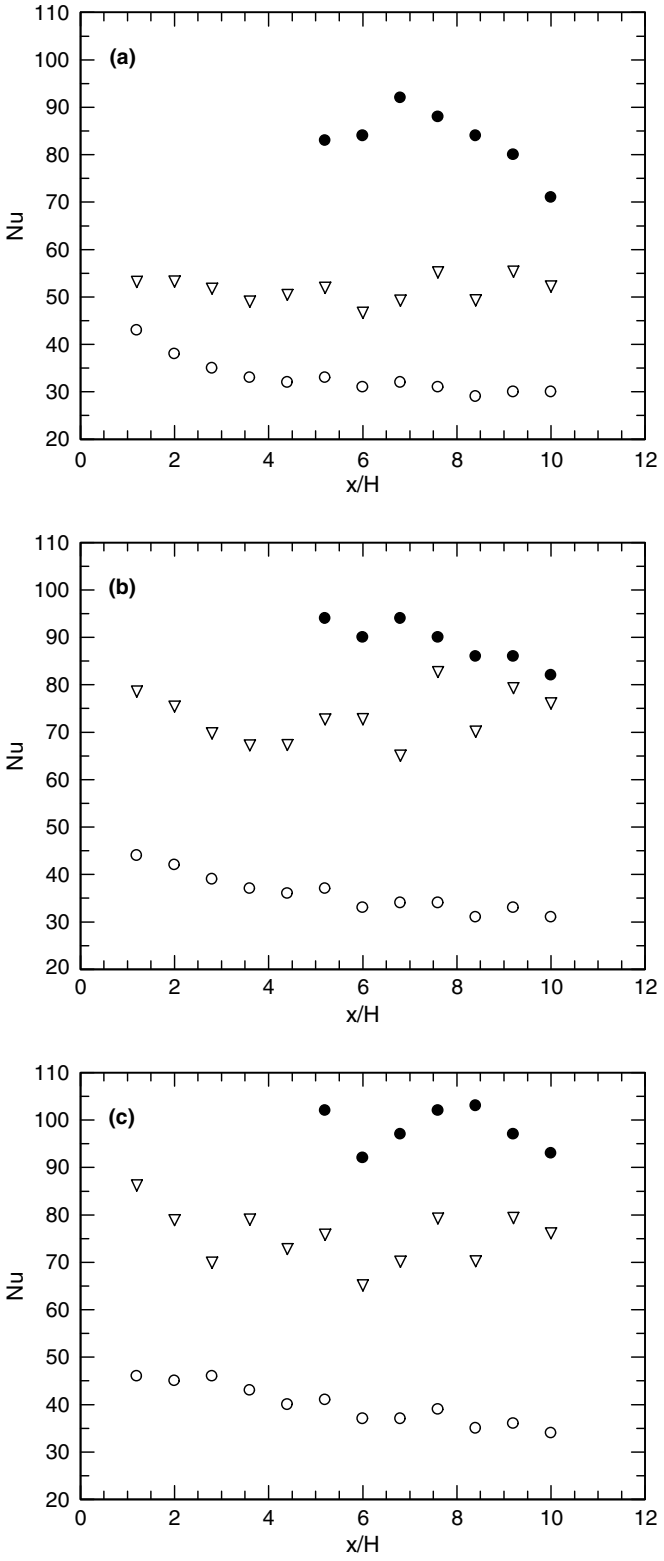

Fig. 10. Comparison of local Nusselt number before and after the use of vortex generators. ▽, 0 ppm (without generators); ○, 90 ppm (without generators); ●, 90 ppm (with generators). $Re = 7000$ (a); 12,000 (b); 16,200 (c).

Table 1
Averaged Nusselt numbers obtained under various conditions

Re	*c*					
	0 ppm	30 ppm	70 ppm	80 ppm	90 ppm	90 ppm (with vortex generators)
7000	54.7	51.6	44.6	32.2	29.7	83.2
12,000	72.9	70.0	50.0	33.3	34.0	89.0
16,200	78.4	74.5	64.0	41.9	39.4	98
18,500	87.7	82.3	81.8	52	41.0	–

stress; the flow far from the vortex generators tends to recover as drag-reducing flow because the high shear stress does not last a long distance downstream of the vortex generators. Therefore, to achieve satisfactory heat transfer enhancement over the whole surface of a long heat exchanger, extra rows of vortex generators downstream may be needed. For the convenience of comparing the heat transfer rate under various conditions, the Nusselt numbers at different surfactant concentrations averaged over $x/H = 2$–10 without the vortex generators and those averaged over $x/H = 5$–10 with the vortex generators for the case of 90 ppm are summarized in Table 1.

The pressure drop penalty due to the use of the vortex generators over the heating surface is assessed by comparing the measured pressure difference at the pressure tapping points separated by a distance of 0.4 m with that measured without the use of vortex generators. It is found that at $Re = 7000$, the pressure drop is about 10% higher than that without the application of the vortex generators. This value is increased to 25% when *Re* is increased to 16,200. The present result seems to indicate that the pressure drop penalty is very small compared with those reported previously [11–13].

In comparison with the results of previous investigations for heat transfer enhancement in a drag-reducing flow, the effectiveness of the present technique is found to be better. For example, Eschenbacher et al. [13] with a triangular winglet mounted on the flat heating surface were only able to recover the heat transfer to the level similar to the case without surfactant (with $Nu \approx 55$) at Reynolds number of 7000. On the other hand, the heat transfer rate in the present study is enhanced ($Nu \approx 85$) to a level which is about 52% higher than that for tap water. Li et al. [12] used three types of wire-meshes inserted in the channel to enhance the heat transfer rate in the drag-reducing flow. The maximum attainable heat transfer enhancements are about 200% as compared to the case without the enhancement device. However, the use of the wire mesh may result in a large pressure drop along the channel. This may restrict its use in practical applications. Furthermore, such a high enhancement rate obtained by Li et al. [12] is achievable only at high Reynolds numbers (e.g. $Re \geqslant 22{,}000$). For Reynolds numbers lower than this value, the shear stress in the flow may not be high enough to break down the orderly aligned rod-like micelles. The method used by Qi et al. [11] is to provide continuous disturbance to the viscous boundary layer near the solid wall so that the heat transfer ability of the drag-reducing fluid can be enhanced. They found that for the Ethoquad T13-50/NaSal (5 mM/8.75 mM) surfactant solution, the fluted tube-in-tube heat exchanger has a Nusselt number which is 1.2 times that of water in smooth tube. However, due to the high pressure drop penalty, the practical use of fluted tubes to enhance the heat transfer ability depends on the details of the circulation system. For the surfactant solution SPE98330 (1500 ppm), the heat transfer enhancement is at least 1.4 times that of water in straight tubes with pressure drop in the fluted tube being only about 2 times that of water in fluted tube at low Reynolds numbers. When Reynolds number is increased, the pressure drop is near or even lower than that of water in the fluted tube. These latter results are comparable with those obtained in the present study.

4. Conclusions

Drag reduction was examined for four different surfactant concentrations, namely 30, 70, 80 and 90 ppm over a Reynolds number range of 7000–18,500. The maximum achievable drag reductions for different surfactant concentrations are 7%, 30%, 50% and 54%, respectively. The critical Reynolds number for decrease of drag reduction increases with the increase in surfactant concentration, changing from 12,000 at 70 ppm to 17,000 at 90 ppm. The heat transfer reduction was examined for surfactant concentrations of 0, 30, 70, 80 and 90 ppm, respectively, over the same Reynolds number range as that for drag reduction. At all these Reynolds numbers, there is no apparent reduction of heat transfer with 30 ppm of surfactant. At $Re = 7000$, the heat transfer reduction is only about 18% when 70 ppm of surfactant is added to the flow. By increasing the surfactant concentration to 80 and 90 ppm, significant heat transfer reductions (~45%) are noted. When Reynolds number is increased to higher values, the heat transfer rate in reduced by about 45–55% for 80 and 90 ppm. A row of low-profile vortex generators were used to enhance the heat transfer rate for a surfactant concentration of 90 ppm at $Re = 7000$, 12,000 and 16,200. The results show that the averaged Nusselt number is enhanced by 180%, 160% and 150%, respectively for the above three Reynolds numbers as compared with that obtained in the surfactant solution. The present results have also shown that the heat transfer rate is enhanced by 25–52%, relative to that obtained in tap water without

the use of the vortex generators with only a small pressure drop penalty.

Acknowledgements

The authors wish to acknowledge the financial support from Ministry of Education of Singapore through the Academic Research Fund RG13/02. T. Zhou wishes to thank J.J. Wang for useful discussion.

References

[1] B.A. Toms, Some observations on the flow of linear polymer solutions through straight tubes at large Reynolds number, in: Proceedings of 1st International Congress on Rheology, vol. 2, Amsterdam, 1948, pp. 135–141.
[2] A. Gyr, H.-W. Bewersdorff, Drag Reduction of Turbulent Flows by Additives, Kluwer Academic Publishers, The Netherlands, 1995.
[3] J.L. Zakin, B. Lu, H.W. Bewerslorff, Surfactant drag reduction, Rev. Chem. Eng. 14 (4–5) (1998) 255–320.
[4] M. Poreh, U. Paz, Turbulent heat transfer to dilute polymer solutions, Int. J. Heat Mass Transfer 11 (1968) 805–810.
[5] Y.I. Cho, J.P. Hartnett, Non-Newtonian fluids in circular pipe flows, Adv. Heat Transfer 15 (1982) 60–141.
[6] K. Gasljevic, E.F. Matthys, On saving pumping power in hydronic thermal distribution systems through the use of drag-reducing additives, Energy Build. 20 (1993) 45–56.
[7] J.L. Zakin, B. Lu, H.W. Bewersdorff, Surfactant drag reduction, Rev. Chem. Eng. 14 (4–5) (1998) 253–320.
[8] G. Aguilar, K. Gasljevic, E.F. Matthys, Coupling between heat and momentum transfer mechanism for drag-reducing polymer and surfactant solutions, J. Heat Transfer 121 (1999) 796–802.
[9] G. Aguilar, K. Gasljevic, E.F. Matthys, Asymptotes of maximum friction and heat transfer reductions for drag-reducing surfactant solutions, Int. J. Heat Mass Transfer 44 (2001) 2835–2843.
[10] M. Fossa, L.A. Tagliafico, Experimental heat transfer of drag-reducing polymer solutions in enhanced surface heat exchangers, Exp. Thermal Fluid Sci. 10 (1995) 221–228.
[11] Y.Y. Qi, Y. Kawaguchi, Z.Q. Lin, M. Ewing, R.N. Christensen, J.L. Zakin, Enhanced heat transfer of drag reducing surfactant solutions with fluted tube-in-tube heat exchanger, Int. J. Heat Mass Transfer 44 (2001) 1495–1505.
[12] P.W. Li, Y. Kawaguchi, H. Daisaka, A. Yabe, K. Hishida, M. Maeda, Heat transfer enhancement to the drag-reducing flow of surfactant solution in two-dimensional channel with mesh-screen inserts at the inlet, J. Heat Transfer 123 (2001) 779–789.
[13] J.F. Eschenbacher, M. Joko, K. Nakabe, K. Suzuki, Heat transfer in the wake behind a longitudinal vortex generator immersed in drag-reducing channel flows, Int. J. Transport Phenom. 4 (2002) 262–269.
[14] Y. Kawaguchi, T. Segawa, Z.P. Feng, P.W. Li, Experimental study on drag-reducing channel flow with surfactant additives-spatial structure of turbulence investigated by PIV system, Int. J. Heat Fluid Flow 23 (2002) 700–709.
[15] Y.Y. Qi, Y. Kawaguchi, R.N. Christensen, J.L. Zakin, Enhancing heat transfer ability of drag reducing surfactant solutions with static mixers and honeycombs, Int. J. Heat Mass Transfer 46 (2003) 5161–5173.
[16] F.B. Hsiao, C.F. Liu, J.Y. Shyu, Control of wall-separated flow by internal acoustic excitation, AIAA J. 28 (1990) 1440–1446.
[17] M. Yamaguchi, H. Sugawara, H. Usui, H. Suzuki, A study on cationic surfactants as drag reducing additives, AIChE Annual Meeting, Dallas, TX, 1999.
[18] A. Glezer, M. Amitay, Synthetic jets, Ann. Rev. Fluid Mech. 34 (2002) 503–529.
[19] A. Glezer, Shear flow control using fluidic actuator technology, in: Proceedings of the 1st Symposium on Smart Control of Turbulence, Tokyo, 1999.
[20] G. Kravchenko, H. Choi, P. Moin, On the relation of near-wall streamwise vortices to wall skin friction in turbulent boundary layers, Phys. Fluids 5 (1993) 3307–3309.
[21] H. Choi, P. Moin, J. Kim, Active turbulence control for drag reduction in wall-bounded lows, J. Fluid Mech. 262 (1994) 75–110.
[22] C. Lee, J. Kim, H. Choi, Suboptimal control of turbulent channel flow for drag reduction, J. Fluid Mech. 358 (1998) 245–258.
[23] S.K. Robinson, Coherent motions in the turbulent boundary layer, Ann. Rev. Fluid Mech. 23 (1991) 601–639.
[24] D.C. McCormick, Shock-boundary layer interaction control with low-profile vortex generators and passive cavity. AIAA Paper, 30th AIAA Aerospace Sciences Meeting and Exhibit, Reno, NV, 6–9 January 1992.
[25] K. Torii, K.M. Kwak, K. Nishino, Heat transfer enhancement accompanying pressure-loss reduction with winglet-type vortex generators for fin-tube heat exchangers, Int. J. Heat Mass Transfer 45 (2002) 3795–3801.
[26] J.C. Lin, Review of research on low-profile vortex generators to control boundary-layer separation, Prog. Aerospace Sci. 38 (2002) 389–420.
[27] S.J. Kline, F.A. McClintok, Describing uncertainties in single-sample experiments, Mech. Eng. 75 (1953) 3–8.
[28] H. Tennekes, J.L. Lumley, A First Course in Turbulence, MIT Press, 1972.
[29] K. Gasljevic, G. Aguilar, E.F. Matthys, An improved diameter scaling correlation for turbulent flow of drag-reducing polymer solutions, J. Non-Newtonian Fluid Mech. 84 (1999) 131–148.
[30] K. Gasljevic, G. Aguilar, E.F. Matthys, On two distinct types of drag-reducing fluid, diameter scaling, and turbulent profiles, J. Non-Newtonian Fluid Mech. 96 (2001) 405–425.
[31] F.C. Li, Y. Kawaguchi, K. Hishida, Investigation on heat transfer characteristics of drag-reducing flow with surfactant additive by simultaneous measurements of temperature and velocity fluctuations in thermal boundary layer, in: Proceedings of the 6th ASME–JSME Thermal Engineering Joint Conference, Hawaii, March 2003.
[32] D. Ohlendorf, W. Interthal, H. Hoffmann, Surfactant system for drag reduction: physico-chemical properties and rheological behavior, Rheol. Acta 25 (1986) 468–486.
[33] V. Gnielinski, New equations for heat and mass transfer in turbulent pipe and channel flow, Int. Chem. Eng. 16 (1976) 359–368.
[34] K. Gasljevic, E.F. Matthys, Experimental investigation of thermal and hydrodynamic development regions for drag-reducing surfactant solutions, J. Heat Transfer 119 (1997) 80–88.